導電帶與價電帶井深比例對405-nm氮化銦鎵量子井雷射特性之影響

劉柏挺、郭艷光、顏勝宏、林正洋

摘要

本文以數值計算來探討導電帶與價電帶井深比例對405-nm氮化銦鎵量子井雷射特性的影響。特別是導電帶與價電帶井深比例爲7/3的$In_xGa_{1-x}N/In_yGa_{1-y}N$異質結構的光學特性。比較顯示現今大家所認同的井深比例爲7/3比2002年以前一般所認同的井深比例爲3/7有較佳的雷射效能及在量子井有較均勻的載子濃度分布。本文亦由模擬的結果推導出405 nm雷射結構在一些特定銦含量的披覆層時，其量子井厚度與量子井銦含量的關係式，以作爲設計的參考。

關鍵字：氮化銦鎵、導電帶與價電帶井深比例、量子井雷射、臨界電流。

劉柏挺：修平技術學院機械工程系助理教授
郭艷光：彰化師範大學物理系副教授
顏勝宏：彰化師範大學物理研究所碩士班研究生
林正洋：彰化師範大學光電科技研究所碩士班研究生

Effect of Band-Offset Ratio on Characteristics of 405-nm InGaN Quantum-Well Lasers

Bo-Ting Liou, Yen-Kuang Kuo, Sheng-Horng Yen, Cheng-Yang Lin

Abstract

The effect of band-offset ratio on the characteristics of the 405-nm InGaN quantum-well lasers is studied numerically. Specifically, the optical properties are investigated when the band-offset ratio of the $In_xGa_{1-x}N/In_yGa_{1-y}N$ heterojunction is 7/3. Compared to a band-offset ratio of 3/7, which was widely accepted before the year 2002, the laser performance is better and the distribution of carrier concentration in the quantum wells becomes more uniform when the band-offset ratio is 7/3, which is accepted by most researchers recently. Several formulae are derived from simulations, which can be used as a handy tool to calculate the thickness of $In_xGa_{1-x}N$ well layer in the 405-nm laser structure for specific indium compositions of $In_xGa_{1-x}N$ well layer and $In_yGa_{1-y}N$ barrier layer.

Key Words：InGaN, Band-Offset Ratio, Quantum-Well Laser, Threshold Current.

Bo-Ting Liou: Assistant Professor, Department of Mechanical Engineering, Hsiuping Institute of Technology.
Yen-Kuang Kuo: Associate Professor, Department of Physics, National Changhua University of Education.
Sheng-Horng Yen: Graduated Student, Department of Physics, National Changhua University of Education.
Cheng-Yang Lin: Graduated Student, Institute of Photonics, National Changhua University of Education

1. Introduction

III-nitride semiconductors have received much attention in the past few years due to their potential applications in light-emitting diodes, full-color displays, and laser diode light sources for high-density optical storage systems. Specifically, the 405-nm laser diode can be applied to the next-generation optical disc systems with high-density capacity of 22.5 GB as a light source for reading signals [1—9]. The InGaN ternary semiconductor compounds are most commonly used as violet-blue laser diodes active-layer materials [10—13]. Previously, such material encountered several problems in lattice mismatch substrate, high-dislocation densities, and difficulty in obtaining high-quality, low-resistivity *p*-type claddings. To overcome these problems, sapphire or SiC substrates have been utilized for the epitaxial growth of nitrides. InGaN multiple quantum-well (MQW) structures grown on an epitaxially laterally overgrown GaN (ELOG) substrate were further proven to have an estimated lifetime of more than 10000 h under continuous-wave operation at 20 ℃ [14].

An AlGaN blocking layer above the active region is commonly employed to solve the problems of electronic current overflow and dissociation of InGaN well layer during crystal growth at a high temperature of 750 ℃. However, although the AlGaN blocking layer is helpful in electrons confinement, it hinders holes from moving into the active layer and causes deterioration of the non-uniform hole distribution [12]. The electronic current overflow and non-uniform carrier distribution are closely relevant to the band offset of quantum-well heterostructures [15—19]. Before the year 2002, a band-offset ratio of 3/7 [15,20,21], or around 4/6 [22,23], was widely accepted for the $In_xGa_{1-x}N/In_yGa_{1-y}N$ heterojunction. Under these specific circumstances, the electronic current overflow occurs mainly because of the relatively small band offset in the conduction band. On the other hand, the non-uniform hole distribution occurs easily, mainly because of the high effective mass of hole and the high band offset in the valence band. Quite

recently, band-offset ratios of 8/2 [24,25], 7.5/2.5 [26—28], around 7/3 [29—32], and around 6/4 [33,34] have been proposed by different researchers. The average of these newly proposed band-offset ratios is about 7/3. Under these circumstances, the band-offset ratio is larger than one, and the optical properties of the InGaN laser diode structures could be very different from when the band-offset ratio is smaller than one.

In this article, assuming that the band-offset ratio has a value of 7/3, the LASTIP (abbreviation of LASer Technology Integrated Program) simulation program is utilized to numerically investigate the laser characteristics of the 405-nm InGaN quantum-well lasers. Detailed comparisons between the results obtained with a band-offset ratio of 3/7 and those obtained with a band-offset ratio of 7/3 are reported. Specifically, the electronic current overflow, the stimulated recombination rate, the distribution of electrons and holes in the quantum wells, and the laser characteristics for various structural parameters in the active layer are investigated.

2. Laser structure and parameters

A schematic diagram of the InGaN laser diode structure under study is shown in Fig. 1, which is referred to real structures grown in labs [35—37]. It is assumed that the InGaN laser diode structure is grown on an *n*-type GaN layer, which has a thickness of 3 μm. On top of this GaN layer is a 0.1-μm-thick n-type $In_{0.1}Ga_{0.9}N$ layer and a 1.3-μm-thick *n*-type $Al_{0.07}Ga_{0.93}N$ cladding layer, followed by a 0.1-μm-thick *n*-type GaN guiding layer. The active region of the laser diode structure under study consists of undopped $In_{0.12}Ga_{0.88}N/In_{0.02}Ga_{0.98}N$ quantum wells and barriers, which have a thickness of 2.7 nm and 7 nm, respectively. A 0.02-μm-thick *p*-type $Al_{0.2}Ga_{0.8}N$ blocking layer is grown on top of the active region, followed by a 0.1-μm-thick *p*-type GaN guiding layer and a 1.3-μm-thick *p*-type $Al_{0.07}Ga_{0.93}N$ cladding layer. Finally, a 0.05-μm-thick *p*-type GaN cap layer is grown to complete the structure. The doping con-

centration is 1×10^{18} cm^{-3} for all *n*- and *p*-type layers. The active region is 5 μm in width and 500 μm in length. The reflectivities of the two end facets are set at 70% and 90%, respectively [38].

The band gap energy of $In_xGa_{1-x}N$ ternary alloy can be expressed by the following formula [16,17]:

$$E_g(x) = x \cdot E_{InN} + (1-x) \cdot E_{GaN} - b \cdot x \cdot (1-x) \quad (1)$$

where *Eg(x)* is the band gap energy of $In_xGa_{1-x}N$, E_{InN} is the band gap energy of InN that has a value of 0.77 eV, E_{GaN} is the band gap energy of GaN that has a value of 3.42 eV, and *b* is the band gap bowing parameter of $In_xGa_{1-x}N$ that has a value of 1.4 eV [39].

The effective masses of electrons and holes used in simulation are

$$m_{e,In_xGa_{1-x}N} = m_{e,GaN} + x(m_{e,InN} - m_{e,GaN}), \quad (2)$$

$$m_{hh,In_xGa_{1-x}N} = m_{hh,GaN} + x(m_{hh,InN} - m_{hh,GaN}), \quad (3)$$

$$m_{lh,In_xGa_{1-x}N} = m_{lh,GaN} + x(m_{lh,InN} - m_{lh,GaN}) \quad (4)$$

where $m_{e,InxGa1-xN}$ is the effective mass of electrons in $In_xGa_{1-x}N$, $m_{hh,InxGa1-xN}$ and $m_{lh,InxGa1-xN}$ are the effective masses of heavy holes and light holes in $In_xGa_{1-x}N$, respectively, $m_{e,InN}$ (= $0.1\times m_0$) and $m_{e,GaN}$ (= $0.151\times m_0$) are the effective masses of electrons in InN and GaN, respectively, $m_{hh,InN}$ (= $1.449\times m_0$) and $m_{hh,GaN}$ (= $1.595\times m_0$) are the effective masses of heavy holes in InN and GaN, respectively, $m_{lh,InN}$ (= $0.157\times m_0$) and $m_{lh,GaN}$ (= $0.261\times m_0$) are the effective masses of light holes in InN and GaN, respectively, and m_0 is the electron mass in free space [40].

3. Results and discussion

As mentioned previously, an AlGaN blocking layer is commonly employed to solve the problems of electronic current overflow and dissociation of InGaN well layer during crystal growth. We first investigate the effect of different *p*-$Al_xGa_{1-x}N$ blocking layers on the electronic overflow current for $In_{0.12}Ga_{0.88}N/In_{0.02}Ga_{0.98}N$ triple quantum-well (TQW) laser structure when the band-offset ratios are 3/7 and 7/3. From the emission spectra (not shown), the laser wavelengths are determined to be 410 nm

and 405 nm when the band-offset ratios are 3/7 and 7/3, respectively. When the band-offset ratio of the $In_{0.12}Ga_{0.88}N/In_{0.02}Ga_{0.98}N$ heterojunction is 7/3, the laser wavelength has a blue shift of 5 nm compared to when the band-offset ratio is 3/7. This is due mainly to the increased band offset in the conduction band.

Figure 2 shows the overflow current as a function of the input current at different aluminum compositions in the AlGaN blocking layer of the $In_{0.12}Ga_{0.88}N/In_{0.02}Ga_{0.98}N$ TQW laser structure when the band-offset ratios are 3/7 and 7/3. The electronic overflow current is decreased dramatically when the aluminum composition in the AlGaN blocking layer is increased. When the band-offset ratio is 7/3, the relatively high band offset in the conduction band is beneficial for electrons confinement, which results in small electronic overflow current. Note that, for a ratio of 3/7 as shown in Fig. 2a, the electronic overflow current is negligible when the aluminum composition in the AlGaN blocking layer is larger than 0.1. Similarly, for a ratio of 7/3 as shown in Fig. 2b, the electronic overflow current is negligibly small when the aluminum composition in the AlGaN blocking layer is 0.06. However, in order to simulate most real cases of crystal growth, the aluminum composition in the AlGaN blocking layer is set to be 0.2 for following studies.

Figure 3 shows the laser output power as a function of the input current, i.e., the L-I curve, for the laser structure with different numbers of $In_{0.12}Ga_{0.88}N/In_{0.02}Ga_{0.98}N$ quantum wells when the band-offset ratios are 3/7 and 7/3. The threshold currents for the band-offset ratio of 7/3 are lower than those for the band-offset ratio of 3/7. Since the electronic current overflow is almost negligible when the aluminum composition in the AlGaN blocking layer is equal to 0.2, the results are due mainly to the non-uniform hole distribution caused by the high effective mass of hole and the high band offset in the valence band for the band-offset ratio of 3/7. It is inferred from Fig. 3 that, the $In_{0.12}Ga_{0.88}N/In_{0.02}Ga_{0.98}N$ double quantum-well (DQW) laser structure has

the lowest threshold currents of 217.1 mA (= 8.68 kA/cm^2) and 92.3 mA (= 3.69 kA/cm^2) for the band-offset ratios of 3/7 and 7/3, respectively.

Figure 4 shows the stimulated recombination rates of the $In_{0.12}Ga_{0.88}N/In_{0.02}Ga_{0.98}N$ single quantum-well (SQW), DQW, and TQW laser structures at an input current of 400 mA when the band-offset ratios are 3/7 and 7/3. For the band-offset ratio of 3/7, as shown in Fig. 4a, the stimulated recombination rates for the SQW and DQW laser structures are positive in all quantum wells. The total stimulated recombination rate for the DQW laser structure is larger than that for the SQW laser structure. As for the TQW laser structure, the right well, i.e., the one close to the p side, and the central well have relatively small stimulated recombination rates, and the left well, i.e., the one close to the n side, has negative stimulated recombination rate because there are very few holes in the left well. In other words, the left well does not contribute to stimulated emission; instead, it absorbs light. This is one of the main causes for the increase in threshold current in MQW laser diode structures when the number of InGaN well layers is increased.

For the band-offset ratio of 7/3, as shown in Fig. 4b, the stimulated recombination rates are all positive in the quantum wells. In the DQW and TQW laser structures, the left wells have higher stimulated recombination rates when compared with the right wells. Due to the high band offset in the conduction band, the electrons have a difficulty transporting from the left wells to the right wells. It is also indicated in Fig. 4b that the total stimulated recombination rates of both DQW and TQW laser structures are larger than that of SQW laser structure when the band-offset ratio is 7/3. Moreover, from Figs. 4a and 4b we note that the stimulated recombination rates for the band-offset ratio of 7/3 are much larger than those for the band-offset ratio of 3/7 for SQW, DOW, and TQW laser structures. Hence, it is expected that the laser structures with a band-offset ratio of 7/3 should have better laser performance compared to those with a band-offset ratio of 3/7.

Figure 5 shows the electron and hole concentration distributions of the $In_{0.12}Ga_{0.88}N/In_{0.02}Ga_{0.98}N$ DQW laser structure at an input current of 400 mA when the band-offset ratios are 3/7 and 7/3. It is evident that, for the band-offset ratio of 3/7, due to the use of an AlGaN blocking layer and the relatively high band offset in the valence band, the right well has higher electron and hole concentrations when compared with the left well. For the band-offset ratio of 7/3, the electron and hole concentrations in the quantum wells are quite uniform, except that the right well has a little lower electron concentration when compared with the left well (Fig. 5a), due mainly to the relatively high band offset in the conduction band.

The simulated results of the L-I performance, stimulated recombination rate, and carrier concentration distributions suggest that the DQW laser structure possesses the best laser performance for 405-nm InGaN quantum-well lasers. In fact, the emission wavelength is dependent on the structural parameters in the active layer, such as the indium compositions of well and barrier layers and the thickness of well layers. With a band-offset ratio of 7/3, Fig. 6 shows the thickness of $In_xGa_{1-x}N$ well layer of the 405-nm laser structures as a function of the indium composition of well layer with different indium compositions in $In_yGa_{1-y}N$ barrier layers when the thickness of barrier layer is set to 7 nm. It is found that, to fix the laser wavelength at 405 nm, the thickness of well layer decreases with an increase in indium composition of well and barrier layers under the conditions of this specific simulation. In formulae (5) to (8), the simulated results shown in Fig. 6 are best fitted with the third-order polynomials when the indium composition of barrier layer is 0.02, 0.03, 0.04, and 0.05, respectively,where d is the thickness of $In_xGa_{1-x}N$ well layer at which the laser structure can emit light with a wavelength of 405 nm, and x is the indium composition of $In_xGa_{1-x}N$ well layer. These formulae can be used as a handy tool to calculate the thickness of $In_xGa_{1-x}N$ well layer in the 405-nm laser structure for specific indium com-

$$d = 155.92 - 3445.3x + 25964x^2 - 65833x^3 \text{ mm}, \quad (5)$$

$$d = 134.92 - 2954.1x + 22121x^2 - 55833x^3 \text{ mm}, \quad (6)$$

$$d = 131.35 - 2873.2x + 21486x^2 - 54167x^3 \text{ mm}, \quad (7)$$

$$d = 126.06 - 2742.4x + 20350x^2 - 50833x^3 \text{ mm}, \quad (8)$$

positions of $In_xGa_{1-x}N$ well layer and $In_yGa_{1-y}N$ barrier layer.

Figures 7 and 8 show the threshold current and slope efficiency of the 405-nm $In_xGa_{1-x}N/In_yGa_{1-y}N$ DQW laser structure as a function of the indium composition of $In_xGa_{1-x}N$ well layer with different indium compositions in $In_yGa_{1-y}N$ barrier layers when the thickness of barrier layer is set to 7 nm. For the range of indium compositions under study, the threshold current decreases and the slope efficiency increases with a decrease in indium composition of $In_yGa_{1-y}N$ barrier layer. Moreover, the lowest threshold current is obtained when the indium composition of $In_xGa_{1-x}N$ well layer is near 0.1, and the highest slope efficiency is obtained when the indium composition of $In_xGa_{1-x}N$ well layer is near 0.11.

It is inferred from Figs. 7 and 8 that the best laser performance is obtained when the indium compositions of well and barrier layers are near 0.1 and 0.02, respectively. For this specific situation, the widths of the $In_{0.1}Ga_{0.9}N$ well layer and the $In_{0.02}Ga_{0.98}N$ barrier layer are 5.2 nm (Fig. 6) and 7 nm, respectively. As shown in Figs. 7 and 8, the $In_{0.1}Ga_{0.9}N/In_{0.02}Ga_{0.98}N$ DQW laser structure has a threshold current of 81.3 mA and a slope efficiency of 0.149 mW/mA.

4. Conclusion

For InGaN quantum-well laser structure, the band-offset ratio is an important parameter on structure design and characteristics analysis of lasers. During the development of InGaN quantum-well laser structure, different band-offset ratios were proposed and used continually. In the recent three years, a ratio larger than one seems to be a consensus among most researchers. In this article, we use a band-

offset ratio of 3/7, which was most frequently used in early times, and a band-offset ratio of 7/3 recently accepted in the majority, to investigate the effect of band-offset ratio on the analysis of the 405-nm InGaN quantum-well laser characteristics. Simulation results indicate that the threshold current is lower and the stimulated recombination rate is higher when the band-offset ratio is changed from 3/7 to 7/3. Moreover, the DQW laser structure has the lowest threshold current for the band-offset ratios of 3/7 and 7/3. When the band-offset ratio is 7/3, the distributions of electron and hole concentrations in the quantum wells of the DQW laser structure are very uniform, except that the right well has a little lower electron concentration when compared with the left well, due mainly to the relatively high band offset in the conduction band.

With a band-offset ratio of 7/3, four formulae are derived from the curve fitting of the thickness of $In_xGa_{1-x}N$ well layer of the 405-nm laser structures as a function of the indium composition of $In_xGa_{1-x}N$ well layer with different indium compositions in $In_yGa_{1-y}N$ barrier layers when the thickness of barrier layer is set to 7 nm. These formulae can be used as a handy tool to calculate the thickness of $In_xGa_{1-x}N$ well layer in the 405-nm laser structure for specific indium compositions of $In_xGa_{1-x}N$ well layer and $In_yGa_{1-y}N$ barrier layer. Simulated results indicate that the best laser performance is obtained when the indium compositions of well and barrier layers are near 0.1 and 0.02, respectively. The $In_{0.1}Ga_{0.9}N/In_{0.02}Ga_{0.98}N$ DQW laser structure has a threshold current of 81.3 mA and a slope efficiency of 0.149 mW/mA.

Acknowledgements

This work is supported by the National Science Council (NSC) of the Republic of China, Taiwan, under grants NSC-92-2112-M-018-008.

References

1. W.-C. Hsu, M.-R. Tseng, S.-Y. Tsai, P.-C. Kuo: Jpn. J. Appl. Phys. 42, 1005 (2003)
2. Y. Sabi, S. Tamada, T. Iwamura, M.

Oyamada, F. Bruder, R. Oser, H. Berneth, K. Hassenruck: Jpn. J. Appl. Phys. **42**, 1056 (2003)

3. M. Shinotsuka, N. Onagi, M. Harigaya: Jpn. J. Appl. Phys. **39**, 976 (2000)
4. J. Ko, I.S. Park, D.-S. Yoon, C.-S. Chung, Y.-G. Kim, M.-D. Ro, T.-Y. Doh, D.-H. Shin: Jpn. J. Appl. Phys. **40**, 1604 (2001)
5. M. Shinotsuka, H. Iwasa, R. Furukawa, S. Murata, M. Abe, Y. Kageyama: Jpn. J. Appl. Phys. **39**, 1693 (2002)
6. T.K. Kim, Y.M. Ahn, T. Otsuka, H.J. Suh, C.S. Chung, C.W. Lee, E. Tanaka: Jpn. J. Appl. Phys. **39**, 1840 (2002)
7. K. Schep, B. Stek, R.V. Woudenberg, M. Blum, S. Kobayashi, T. Narahara, T. Yamagami, H. Ogawa: Jpn. J. Appl. Phys. **40**, 1813 (2001)
8. E.R. Meinders, H.J. Borg, M.R. Lankhorst, J. Hellmig, A.V. Mijiritskii: J. Appl. Phys. **91**, 9794 (2002)
9. D.P. Bour, M. Kneissl, C.G. Van de Walle, G.A. Evans, L.T. Romano, J. Northrup, M. Teepe, R. Wood, T. Schmidt, S. Schoffberger, N.M. Johnson: IEEE J. Quantum Electron. **36**, 184 (2000)
10. T. Ohno, S. Ito, T. Kawakami, M. Taneya: Appl. Phys. Lett. **83**, 1098 (2003)
11. M. Hansen, P. Fini, L. Zhao, A.C. Abare, L.A. Coldren, J.S. Speck, S.P. DenBaars: Appl. Phys.Lett. **76**, 529 (2000)
12. M. Hansen, J. Piprek, P.M. Pattison, J.S. Speck, S. Nakamura, S.P. Denbaars: Appl. Phys.Lett. **81**, 4275 (2002)
13. S. Nakamura, M. Senoh, S. Nagahama, T. Matsushita, H. Kiyoku, Y. Sugimoto, T. Kozaki, H. Umemoto, M. Sano, T. Mukai: Jpn. J. Appl. Phys. **38**, L226 (1999)
14. S. Nakamura, M. Senoh, S. Nagahama, N. Iwasa, T. Yamada, T. Matsushita, H. Kiyoku, Y. Sugimoto, T. Kozaki, H. Umemoto, M. Sano, K, Chocho: Jpn. J. Appl. Phys. **36**, L1568 (1997)
15. K. Domen, R. Soejima, A. Kuramata, T. Tanahashi: MRS Internet J. Nitride Semicond. Res. **3**, 2 (1998)

16. S. Nakamura, G. Fasol: The Blue Laser Diode (Springer-Verlag, Heidelberg 1997)

17.G.B. Stringfellow, M.G. Craford: High Brightness Light Emitting Diodes (Academic Press, San Diego 1997)

18.J.I. Pankove, T.D. Moustakas: Gallium Nitride (GaN) I (Academic Press, San Diego 1998)

19. J.I. Pankove, T.D. Moustakas: Gallium Nitride (GaN) II (Academic Press, San Diego 1999)

20. G. Martin, A. Botchkarev, A. Rockett, H. Morkoc: Appl. Phys. Lett. **68**, 2541 (1996)

21. J. Piprek, R.K. Sink, M.A. Hansen, J.E. Bowers, S.P. Denbaars: Proc. SPIE **3944**, 28 (2000)

22. C.-C. Chen, H.-W. Chung, G.-C. Chi, C.-C. Chuo, J.-I. Chyi: Appl. Phys. Lett. **77**, 3758 (2000)

23. H. Unlu, A. Asenov: J. Phys. D Appl. Phys. **35**, 591 (2002)

24. T. Deguchi, A. Shikanai, K. Torii, T. Sota, S. Chichibu, S. Nakamura: Appl. Phys. Lett. **72**, 3329 (1998)

25. Y.D. Jho, J.S. Yahng, E. Oh, D.S. Kim: Phys. Rev. B **66**, 035334 (2002)

26. J. Dalfors, J.P. Bergman, P.O. Holtz, B.E. Semelius, B. Monemar, H. Amano, I. Akasaki: Appl. Phys. Lett. **74**, 3299 (1999)

27. R.M. Chu, Y.D. Zheng, Y.G. Zhou, S.L. Gu, B. Shen, R. Zhang, R.L. Jiang, P. Han, Y. Shi: Appl. Phys. A **75**, 1 (2002)

28. M.H. Lee, K.J. Kim, E. Oh: Solid State Commun. **123**, 395 (2002)

29. M.S. Minsky, S.B. Fleischer, A.C. Abare, J.E. Bowers, E.L. Hu, S. Keller, S.P. Denbaars: Appl. Phys. Lett. **72**, 1066 (1998)

30. J. Piprek, S. Nakamura, IEE Proc.-Optoelectron. **149**, 145 (2002)

31. C.Y. Lai, T.M. Hsu, W.-H. Chang, K.-U. Tseng, C.-M. Lee, C.-C. Chuo, J.-I. Chyi: J. Appl. Phys. **91**, 531 (2002)

32. A. Kunold, P. Pereyra: J. Appl. Phys. **93**, 5018 (2003)

33. Ch. Manz, M. Kunzer, H. Obloh, A. Ramakrishnan, U. Kaufmann: Appl. Phys. Lett. **74**, 3993 (1999)

34. Y.D. Jho, J.S. Yahng, E. Oh, D.S. Kim: Appl. Phys. Lett. **79**, 1130 (2001)

35. S. Nakamura, M. Senoh, S. Nagahama, N. Iwasa, T. Matsushita, T. Mukai: Appl. Phys. Lett. **76**, 22 (2000)

36. S. Nakamura, M. Senoh, S. Nagahama, N. Iwasa, T. Yamada, T. Matsushita, H. Kiyoku, Y. Sugimoto, T. Kozaki, H. Umemoto, M. Sano, K. Chocho: Appl. Phys. Lett. **72**, 2014 (1998)

37. T. Asano, T. Tojyo, T. Mizuno, M. Takeya, S. Ikeda, K. Shibuya, T. Hino, S. Uchida, M. Ikeda: IEEE J. Quantum Electron. **39**, 135 (2003)

38. M. Kneissl, W.S. Wong, D.W. Treat, M. Teepe, N. Miyashita, N.M. Johnson: IEEE J. Select. Topics Quantum Electron. **7**, 188 (2001)

39. J. Wu, W. Walukiewicz, K.M. Yu, J.W. Ager III, E.E. Haller, H. Lu, W.J. Schaff: Appl. Phys. Lett. **80**, 4741 (2002)

40. D. Fritsch, H. Schmidt, M. Grundmann: Phys. Rev. B **67**, 235205 (2003)

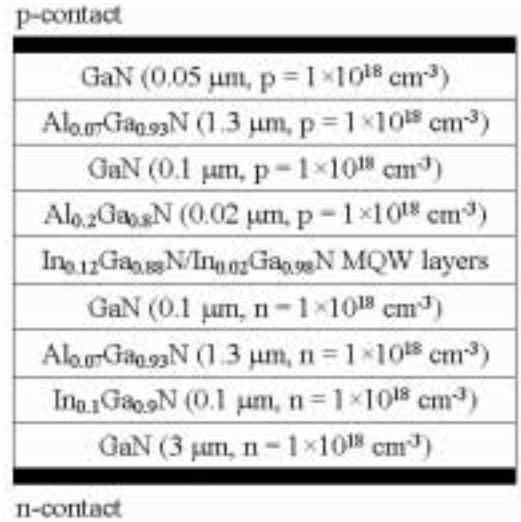

Fig. 1. Schematic diagram of the InGaN laser diode structure under study.

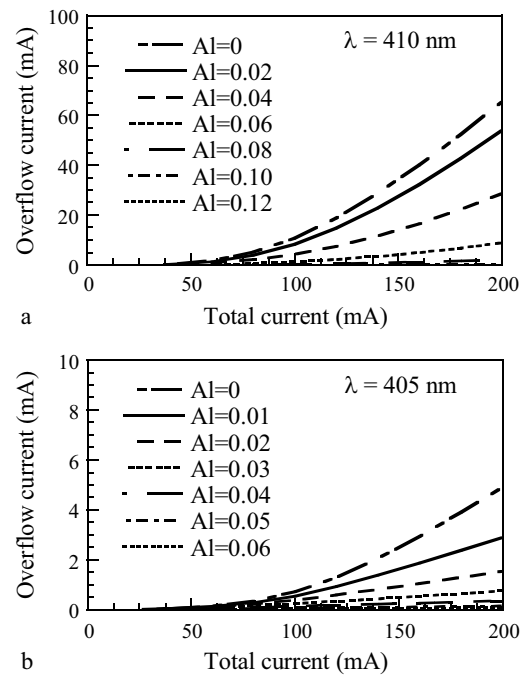

Fig. 2. Overflow current as a function of the input current at different aluminum compositions in the AlGaN blocking layer of the $In_{0.12}Ga_{0.88}N/In_{0.02}Ga_{0.98}N$ TQW laser structure when the band-offset ratios are 3/7 (a) and 7/3 (b).

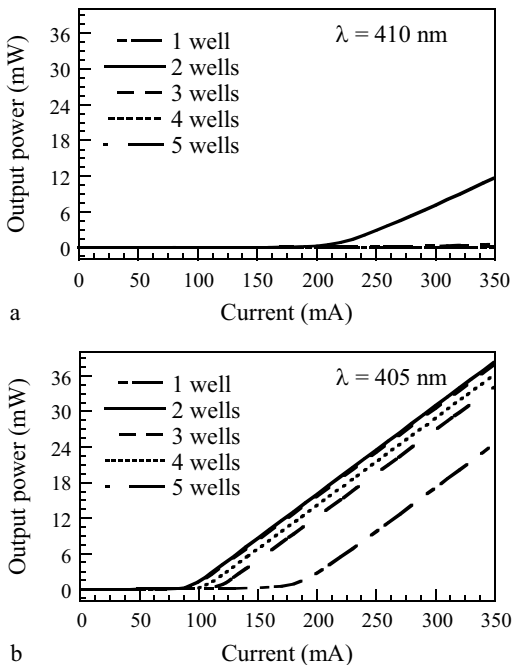

Fig. 3. Laser output power as a function of the input current, i.e., the L-I curve, for the laser structure with different numbers of $In_{0.12}Ga_{0.88}N/In_{0.02}Ga_{0.98}N$ quantum wells when the band-offset ratios are 3/7 (a) and 7/3 (b).

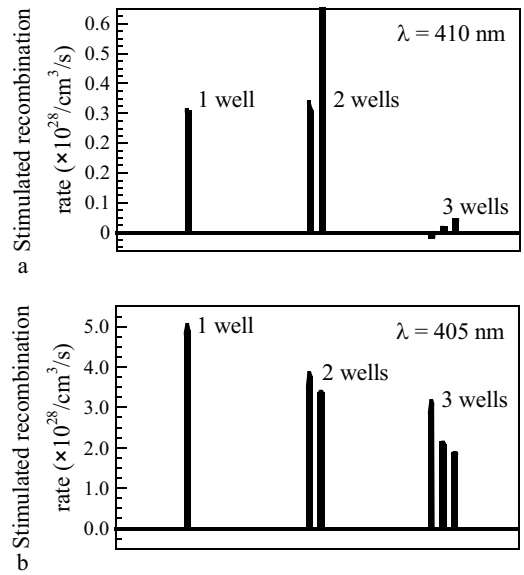

Fig. 4. Stimulated recombination rates of the $In_{0.12}Ga_{0.88}N/In_{0.02}Ga_{0.98}N$ SQW, DQW, and TQW laser structures at an input current of 400 mA when the band-offset ratios are 3/7 (a) and 7/3 (b).

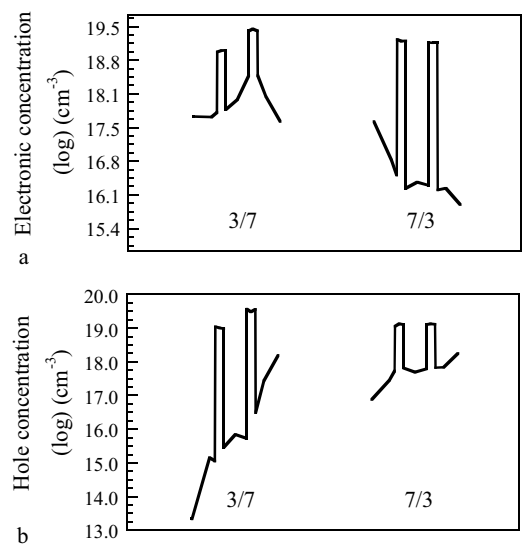

Fig. 5. Electron (a) and hole (b) concentration distributions of the $In_{0.12}Ga_{0.88}N/In_{0.02}Ga_{0.98}N$ DQW laser structure at an input current of 400 mA when the band-offset ratios are 3/7 and 7/3.

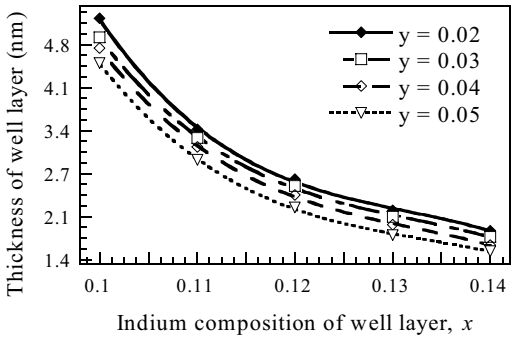

Fig. 6. Thickness of $In_xGa_{1-x}N$ well layer of the 405-nm laser structures as a function of the indium composition of well layer with different indium compositions in $In_yGa_{1-y}N$ barrier layers when the thickness of barrier layer is set to 7 nm.

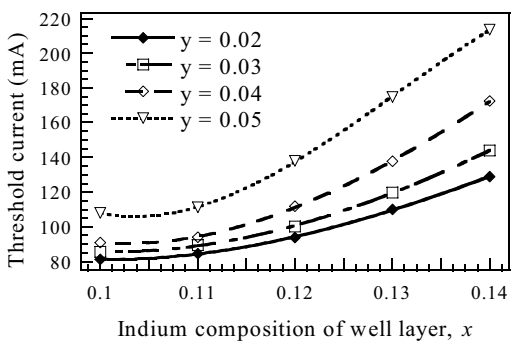

Fig. 7. Threshold current of the 405-nm $InxGa_{1-x}N/In_yGa_{1-y}N$ DQW laser structure as a function of the indium composition of $In_xGa_{1-x}N$ well layer with different indium compositions in $InyGa_{1-y}N$ barrier layers when the thickness of barrier layer is set to 7 nm.

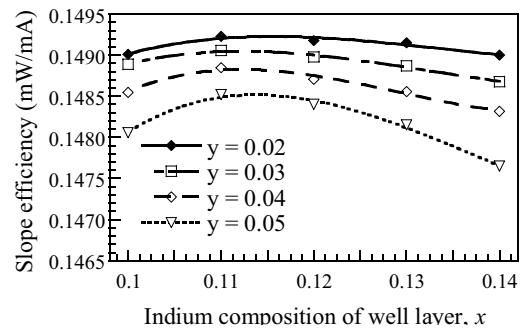

Fig. 8. Slope efficiency of the 405-nm $In_xGa_{1-x}N/In_yGa_{1-y}N$ DQW laser structure as a function of the indium composition of InxGa1-xN well layer with different indium compositions in $In_yGa_{1-y}N$ barrier layers when the thickness of barrier layer is set to 7 nm.